

Digital Interpretability of Annual Tile-based Mosaic of Landsat-8 OLI for Time-series Land Cover Analysis in the Central Part of Sumatra

Ratih Dewanti Dimiyati, Projo Danoedoro, Hartono, Kustiyo and Muhammad Dimiyati

Received:2018-04-27 Accepted: 2018-11-22 / Published online: 2018-12-31
 © 2018 Faculty of Geography UGM and The Indonesian Geographers Association

Abstract This paper presented a digital interpretability of the annual tile-based mosaic (TBM) images for the operational purposes of time-series land cover analysis. The primary data used were the TBM images of Landsat-8 OLI of the central part of Sumatra, acquired from January 2015 to June 2017. The method used was comparing the overall accuracies of the results of the TBM images of land cover classification that using the master training samples of 2016 data with that using the training sample from each year of the three-years of data. The classifications were performed using four groups of spectral bands, namely Band 6-5-4-3-2, Band 6-5-4, Band 6-5-2, and Band 5-4. In order to improve the overall accuracies (OA), the classification results were afterward reclassified using fewer class number, based on Jefferies Matusita (JM) distance approach. The digital interpretability of the images could be deliberated through the average of overall accuracy (AOA) scores, which is Good with a score of > 80%, Fair between 70.0% - 79.9% and Poor if < 70%. The results showed that the use of the group of the Bands 6-5-4-3-2 performed at Good overall accuracy, consistency level with an AOA score of 86% for six object classes. Whereas the classifications using the groups of the Bands 6-5-4-3-2, Bands 6-5-4, and Bands 6-5 indicated Good accuracy, the consistency level for four object classes, with AOA scores of 89%, 82%, and 81%, respectively. It means that the annual mosaic image could be accepted through the digital interpretability of the land cover classification with AOA > 80% for six and four object classes. To support operational requirements, the use of group Bands 6-5 could also be recommended as the most efficient group of bands selected for land cover analysis with four object classes.

Keywords: Overall accuracy, consistency, annual mosaic image, master sample

Abstrak Paper ini menyajikan interpretabilitas digital citra mosaik tahunan TBM untuk keperluan operasional analisis liputan lahan time-series. Data primer yang digunakan yakni citra Landsat-8 OLI TBM wilayah Sumatera bagian tengah, yang direkam dari Januari 2015 hingga Juni 2017. Metode yang digunakan yakni membandingkan akurasi keseluruhan hasil klasifikasi liputan lahan citra TBM menggunakan master training sampel data tahun 2016 dengan hasil klasifikasi menggunakan training sampel dari masing-masing ketiga tahun data. Klasifikasi tersebut dilakukan menggunakan empat kelompok kanal spektral yakni Band 6-5-4-3-2, Band 6-5-4, Band 6-5-2, dan Band 5-4. Guna meningkatkan nilai akurasi keseluruhan, hasil klasifikasi tersebut kemudian dilakukan klasifikasi ulang menggunakan kelas yang lebih sedikit melalui pendekatan Jefferies Matusita (JM) distance. Interpretabilitas citra dapat diukur melalui nilai rata-rata akurasi keseluruhan (AOA), yakni Bagus dengan nilai > 80%, Fair antara 70,0% - 79,9%, dan Buruk apabila < 70%. Hasil penelitian menunjukkan bahwa penggunaan kelompok Band 6-5-4-3-2 mempunyai tingkat konsistensi akurasi keseluruhan Bagus dengan skor AOA 86% untuk enam kelas objek. Sedangkan kelompok Band 6-5-4-3-2, Band 6-5-4, dan Band 6-5 menunjukkan tingkat konsistensi akurasi Bagus untuk empat kelas objek, dengan skor AOA masing-masing yakni sebesar 89%, 82%, dan 81%. Dengan demikian citra mosaik tahunan TBM dapat diterima melalui interpretabilitas digital klasifikasi liputan lahan dengan AOA > 80% untuk enam dan empat kelas objek. Guna mendukung keperluan operasional, penggunaan kelompok Band 6-5 dapat direkomendasikan sebagai kelompok band terpilih paling efisien untuk analisis liputan lahan dengan empat kelas objek. Guna mendukung keperluan operasional, penggunaan kelompok Band 6-5 dapat direkomendasikan sebagai kelompok band terpilih paling efisien untuk analisis liputan lahan dengan empat kelas objek.

Kata kunci: Akurasi keseluruhan, konsistensi, citra mosaik tahunan, sampel master

1. Introduction

Geospatial Data and Information (IG) becomes an important component in national development

planning in Indonesia. Considering the area and the heterogeneity of the region, it is important for Indonesian decision-makers to have accurate and accountable data as a basis for determining the policy direction. The government sets the importance of the One Map Policy (OMP) and is one of the national priority programs outlined in the Nawacita. With One Map Policy, IG will map to One Georeference, One Geo-standard, One Geo-database and One Geocortodian (One Geo-portal) at a map level accuracy of 1: 50,000 or specified scale accuracy (Presiden Republik Indonesia 2016). So far, the problems in national development and regulation are the overlapping of land and the unevenness of

© 2018 by the authors. Licensee Indonesian Journal of Geography, Indonesia.
 This article is an open access article distributed under the terms and conditions of the Creative Commons Attribution (CC BY NC) license <https://creativecommons.org/licenses/by-nc/4.0/>.

Ratih Dewanti Dimiyati
 Gadjah Mada University and LAPAN, Indonesia

Projo Danoedoro and Hartono
 Gadjah Mada University, Indonesia

Kustiyo
 LAPAN, Indonesia

Muhammad Dimiyati
 Directorate General of Strengthening for Research and Development; and University of Indonesia

Correspondent e-mail:

development, caused by the non-standard or unequal maps used as the basis for planning. The perspective of the OMP can be used as leverage in realizing space justice for national development (Presiden Republik Indonesia 2011, 2016). Until now, there are still many non-standard or unequal map uses that have not been referenced in one geospatial reference, one standard, one database, and one geoportal in various sectoral development programs (Presiden Republik Indonesia 2014b).

In addition, there are still many national and regional institutions that have not been supported by the availability of the latest spatial maps. In such areas, the satellite image can be a very useful source of information to complement the availability of spatial data for the implementation of OMP (Presiden Republik Indonesia 2013b, 2018). For areas that are often covered by clouds, such as parts of Kalimantan, Papua, and Sumatra, a model of image processing is required to extract the abundance of imagery data available in the region. The continuity and regularity of the availability of the minimum cloud cover of the annual mosaic image for areas often covered by clouds are necessary for the purposes of regional planning and development (Setiyoko et al, 2016; Kushardono & Dewanti 2016). As a developing country, Indonesia needs the availability and regularity of satellite data covering wide areas to support regional development programs (Presiden Republik Indonesia 2011, 2014a).

Optical remote sensing systems are often constrained by clouds and haze, especially in tropical regions such as Indonesia (Gastellu-Etchegorry 1988; Roswintiarti et al, 2014). But along with the development of data processing technology, some images with different acquisition dates can be processed to produce a cloud-free composite mosaic image through a mosaicing process between cloudy and cloud-free areas. Image mosaicing is the process of combining two or more side-lap/overlap images to produce a representative and continuous image that will be used in a further analysis process for an information extraction need. The principle of this image mosaicing is to replace the cloud and haze covered areas with different scene/tile/pixels with the cloud or haze free data (CRISP 2001; Mougini-mark et al, 2001; Furby 2002; Furby et al, 2006; De Vries et al, 2007; Broich et al, 2011; Ghosh & Kaabouch 2016; Guo et al, 2016; Hansen & Loveland 2012; Roswintiarti et al, 2014; Kustiyo et al, 2015; Kustiyo 2016; Margono et al, 2016).

Several researchers developed solutions to address the availability of medium-scale of remote sensing data in areas often covered by clouds (Roswintiarti et al, 2014), some of them are Pixel-Based Mosaic (PBM) models (Hansen et al, 2008; Kustiyo et al, 2014). In the PBM model, the larger the area being analyzed, the more pixels being processed, or the more time it takes and the more storage capacity it requires. If there are no cloud-free pixels for the region being analyzed, it will be difficult to obtain pixels to replace cloud-

covered areas. Using PBM models often results in less efficiency and makes the complexity of the annual mosaic image analysis process. The Mosaic Tile Based (hereinafter called Tile-Based Mosaic or TBM model) is an approach developed from a set of pixels, so the TBM model can overcome the limitations of the PBM model in making a better accuracy of the annual mosaic image. Thus the TBM model was proposed to be applied in this study. The proposed TBM model was applied to Landsat-8 OLI data in the central part of Sumatra to obtain the minimum cloud cover of the annual TBM image (hereinafter called annual mosaic image). The algorithm of the model was (Dimiyati, RD. et al, 2018):

$$\text{Final_score} = a * \% \text{Cloud Free} + b * \% \text{Haze Free} + c * \% \text{Veg. Conf.} + d * \% \text{Open Land Conv.}$$

Where:

- % Cloud Free is the percentage of brightness value or free from cloud cover on image tile; range of value between 0-100%; 100% value if the tile of cloud free image, and value 0 when the total image tile is closed by cloud;
- % Haze Free is the percentage of brightness or free value of haze on the image tile; the range of values between 0-100%; haze value 100 if the image tile is absolutely no haze, and value 0 if the image tile is completely fogged;
- Veg. Conf. (Vegetation Confidence) is the percentage of a confidence value of the vegetation cover on the image tile, derived from the mean NIR/Green index value on the land; the range of values between 0-100%;
- Open Land Con. (Open Land Confidence) is the percentage of a confidence value of the open land on the image tile, which is derived from the average SWIR-1/Green index value of the land; the range of values between 0-100%; and
- a, b, c, d are coefficients given the value 1.

The purpose of this study was to examine whether the digital interpretability of the annual mosaic image results was acceptable for the digital analysis of time-series land cover. The digital interpretability of data processing is proposed to be measured by the consistency of the annual mosaic image.

The results of this study will be used to ensure that the annual mosaic image of TBM model meets the requirements recommended in the digital interpretability of a digital analysis of time-series land cover image, as an input to the process of standardization of nationwide large-scale remote sensing data processing.

2. The Methods

Study area

The selected study area covered the central part of Sumatra, including parts of Riau, North Sumatra, and West Sumatra Provinces (Figure 1). The main reasons for the selection of this study area are, among others,

that as a part of Indonesia which is often covered by clouds and haze disturbance (Gastellu-Etchegorry 1998; Roswintiarti et al, 2014), and the Landsat-8 OLI images of the TBM model for 2015, 2016, and 2017 are ready for the region (Dimiyati, RD. et al, 2018), and has been shown to have high interpretability for visual land cover analysis (Dimiyati, M. et al, 2018).

In addition, the area has a relatively complete topography and varies, from flat to mountainous. The area also has a relatively complete object of land cover such as forests, swamps, plantations, shrubs, bushes, paddy fields, settlements, and mangroves. The land cover change of the region is quite dynamic and good for representing an analysis of dynamic land cover changes (Broich et al, 2011; Margono et al, 2014; Setiawan et al, 2015).

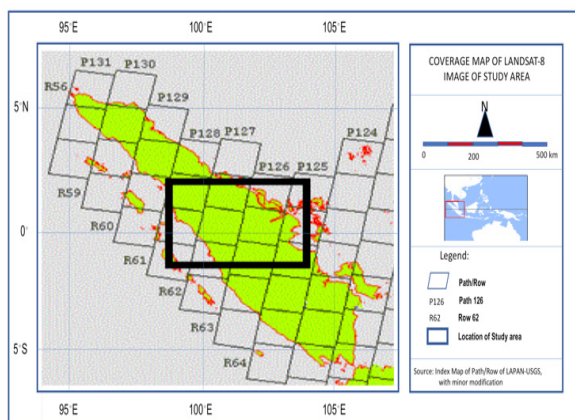


Figure 1. Location and path-row coverage of the study area, the central part of Sumatra

Data

The primary data used for this study were annual mosaic images of Landsat-8 OLI of 2015, 2016, and 2017. Those data have been geometrically corrected at Level-1T (precision and terrain correction level) and radiometrically corrected of ToA (Top of Atmosphere) and BRDF (Bi-directional Reflectance Distribution Function), covering parts of Riau, West Sumatra, and North Sumatra Provinces (Dimiyati, RD. et al, 2018, Dimiyati, M. et al, 2018).

The total data used consisted of 570 scenes, covers 10 (ten) scenes on the path-row 125-59, 125-60, 126-59, 126-60, 126-61, 127-59, 127-60, 127-61, 128-59, and 128-60. However, for three-year data of 2015, 2016, and 2017 in this study, only 478 scenes were used due to the availability at the time of data collection.

The orientation of this study was focused on detecting land cover objects in the terrestrial area. The efficiency and relevancy of using spectral band selection were considered. Several considerations in the spectral band selection where the relevancy to the application theme, sensitivity to land cover and its environment objects, stability to the atmospheric disturbances variability, and avoiding redundancy. The characteristics of spectral bands of Landsat-8 OLI are shown in Table 1. Therefore only 5 (five) spectral bands among 9 (nine) available spectral bands of OLI had been selected for this research (Dimiyati, RD. et al. 2018). The spectral bands selected for this research were Band-2, Band-3, Band-4, Band-5, and Band-6 with spatial resolution of 30 meters. The sensitivity of the five spectral bands to the vegetation and its

Table 1. The characteristics of spectral bands of Landsat-8 OLI (USGS 2015)

Spectral band		Wavelength (μm)	Useful for mapping
Band-1	Coastal Aerosol	0.435 - 0.451	Coastal and aerosol studies.
Band-2	Blue	0.452 - 0.512	Bathymetric mapping, distinguishing soil from vegetation, and deciduous from coniferous vegetation.
Band-3	Green	0.533 - 0.590	Emphasizes peak vegetation, useful for assessing plant vigor.
Band-4	Red	0.636 - 0.673	Discriminates vegetation slopes.
Band-5	Near Infrared (NIR)	0.851 - 0.879	Emphasizes biomass content and shore-lines.
Band-6	Short-wave Infrared (SWIR-1)	1.566 - 1.651	Discriminates moisture content of soil and vegetation; penetrates thin clouds.
Band-7	Short-wave Infrared (SWIR-2)	2.107 - 2.294	Improved moisture content of soil and vegetation and thin cloud penetration.
Band-8	Panchromatic	0.503 - 0.676	15 meter resolution, sharper image definition.
Band-9	Cirrus	1.363 - 1.384	Improved detection of cirrus cloud contamination.

Table 2. The correlation coefficients among spectral bands

		Correlation coefficient (r)			
2015	Band-2	Band-3	Band-4	Band-4	Band-6
Band-2	----	0.98	0.96	0.28	0.63
Band-3	0.98	----	0.98	0.37	0.70
Band-4	0.96	0.98	----	0.28	0.68
Band-5	0.28	0.37	0.28	----	0.71
Band-6	0.63	0.70	0.68	0.71	----
Average	0.71	0.76	0.73	0.41	0.68
2016	Band-2	Band-3	Band-4	Band-4	Band-6
Band-2	----	0.94	0.90	-0.09	0.30
Band-3	0.94	----	0.94	0.09	0.44
Band-4	0.90	0.94	----	-0.07	0.43
Band-5	-0.09	0.09	-0.07	----	0.62
Band-6	0.30	0.44	0.43	0.62	----
Average	0.51	0.60	0.55	0.14	0.45
2017	Band-2	Band-3	Band-4	Band-4	Band-6
Band-2	----	0.94	0.91	-0.02	0.33
Band-3	0.94	----	0.95	0.13	0.47
Band-4	0.91	0.95	----	-0.02	0.45
Band-5	-0.02	0.13	-0.02	----	0.65
Band-6	0.33	0.47	0.45	0.65	----
Average	0.54	0.63	0.57	0.19	0.47

environment is indicated by the high spectral reflectance and the contrast of the objects. Several spectral bands which not directly relevant to the application theme or redundancy being used for this research, such as Band-1, Band-7, Band-8, and Band-9 were skipped in the process. The nearly similar characteristic of Band-6 and Band-7 in the detection of vegetation objects was also considered as redundancy, only one (Band-6) was selected for analysis. Table 2 showed the correlation coefficients among spectral bands of the data used.

Figure 2, Figure 3, Figure 4, and Table 2 were representing spectral characteristics of the reflectance of the data used. The cloud cover of the 2015, 2016, and 2017 TBM data were shown in Figure 2, the cloud variations in the data used were very high and even most of the data used indicated the above 40% cloud cover. The spectral band reflectance statistic parameters such as the mean and standard deviation of each band of the annual TBM images were shown in Figure 3. While the histogram patterns, the tone and object feature differences of each spectral band were shown in Figure 4. From Figure 3 and Figure 4 showed the consistent pattern of reflectance numbers of each spectral band for all three-years of the data, particularly Band-5 (NIR) and Band-6 (SWIR-1). The Band-2, Band-3, and Band-4 look unstable,

particularly the 2015 data which had larger standard deviations compared to the 2016 and 2017 data.

The annual mosaic image Landsat-8 OLI used as the primary data in this study was the image developed using the TBM model with a tile size of 0.02 x 0.02 degrees (2.2 km x 2.2 km). The annual mosaic image included the data from 2015, 2016, and 2017. The 2016 data were used as a reference in the training sample selection for the digital analysis of time-series land cover. The reason for the 2016 data selection was due to the quality of data among the available three-years data, and the availability of the latest reference data from the Ministry of Environment and Forestry (MoEF).

2. The Methods

Three of tile sizes of 0.1 degrees (11x11 km²), 0.05 degrees (5.5x5.5 km²), and 0.02 degrees (2.2x2.2 km²) were used to examine the reliability and simultaneously the level of visual interpretability as well as digital interpretability of the produced images. Of the three tiles, a 0.02x0.02 degree tile had the most optimum accuracy (Dimiyati RD. et al, 2018). The merit of the annual mosaic image could be assessed from the digital interpretability of the product images in particular, for the digital time-series land cover analysis and other analysis. In this study, we proposed the definition of digital interpretability of annual mosaic images,

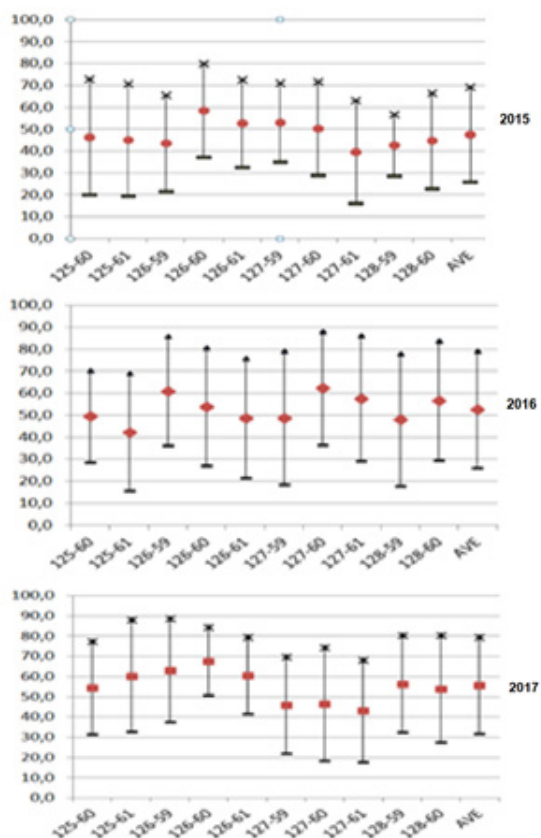


Figure 2. Average cloud cover (%) of the annual mosaic images

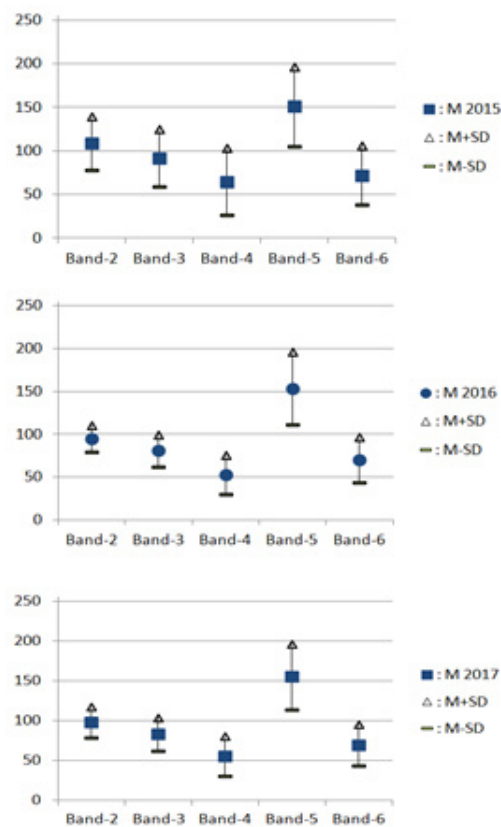


Figure 3. The mean and standard deviation of annual mosaic image reflectance each band

hereinafter called digital interpretability is an automatic image processing quality, which is analyzed by using the master sample. The master sample here is a set of sample statistic training values of a certain year data from the image used. In this study, we proposed the digital interpretability is indicated by the spectral consistency of TBM images for the extraction of annual digital land cover information to answer the question of how many bands are used, which bands, and how many land cover classes can produce the optimal accuracy. The digital interpretability was measured by the accuracies (overall accuracy, user accuracy, and producer accuracy) of the classification results which were analyzed using master sample against the specified reference (Costa et al, 2018; Costachioiu et al, 2011; Danoedoro 2012; Gómez et al, 2016; Islam et al, 2016; Mausel, et al, 1990; Mitchell et al, 2011, 2012; Peacock 2014; Zhongyang et al, 2011).

The procedure to determine the digital interpretability of time-series annual Tile-Based Mosaic (TBM) of Landsat-8 OLI for land cover analysis image consisted of 4 (four) main processes. The main processes consisted of sample selection, image classification, assessment of the object separability and re-classification, and assessment of the accuracy of the digital interpretability. The development steps of digital interpretability through digital time-series land cover classifications were presented in Figure 5.

Sample selection

The master sample selections were completed by identification and delineation of the objects on the red-green-blue (RGB) image of 2016. The clearness of the object and the easiness of object recognition for further analysis could also be identified on the RGB annual mosaic images (Butler 2018; USGS 2018). The training sample selection was also, the supported by using the Land Cover Map produced by the MoEF of 2016 on the scale of 1: 250,000 and the field knowledge. The determination of observed objects in the RGB image of 2016 for digital analysis of time-series land cover was referred to the Indonesia National Standards on Land Cover Classification, Forest Cover Change Calculation Method Based on Visual Optical Remote Sensing Image, and Land cover classes for the interpretation of the medium-resolution optical images (BSN 2010, 2014, 2015). The statistic parameters of the master training sample of 2016, such as mean, deviation standard, variance, and covariance are used for digital classification of time-series land cover of the three-years' data. The observed objects of the master training sample refer to the national land cover classification of the above mentioned standards. The steps of 1, 3, and 4 in Figure 5 represented this process.

Image classification

Digital analysis of time-series land cover of the

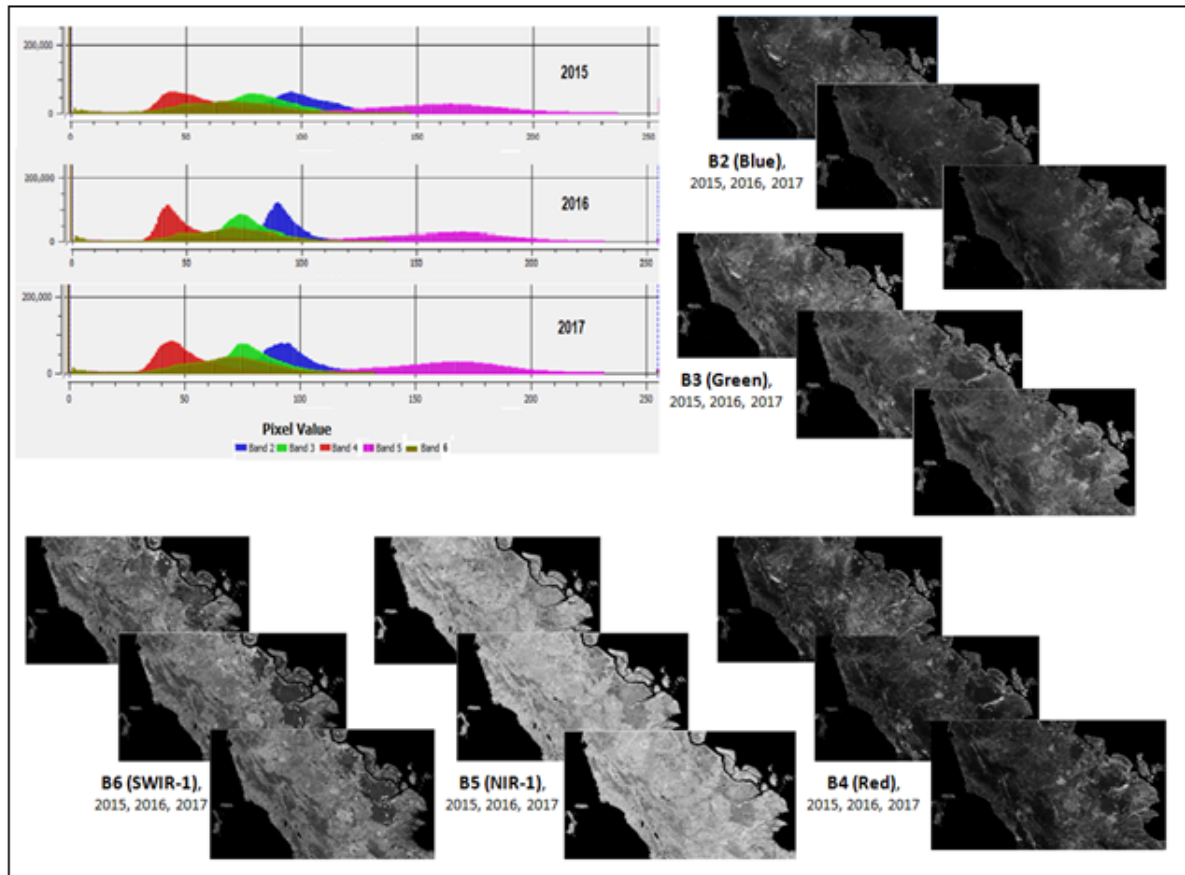


Figure 4. The histogram patterns, and the quick-look of the TBM images showing the tone and object feature differences of each spectral band

annual mosaic images, for the three-years data of 2015, 2016, and 2017 was processed by Maximum Likelihood Classification (MLC) using a set of the master training sample statistic parameters of the annual mosaic image of 2016. The land cover classifications using MLC were examined for each of four groups of the spectral bands, namely (a) Bands 6-5-4-3-2, (b) Bands 6-5-4, (c) Bands 6-5-2, and (d) Bands 6-5. Examination of the spectral band groupings were objected to find the optimum accuracy with the most efficient spectral band numbers among the four spectral band groups (Danoedoro, 2012; Richards & Jia, 2006). Correlation analyses were performed to determine the most optimal spectral band combinations for the digital analysis of time-series land cover classification (Bodart et al., 2011; Ma et al., 2017). The steps of 2 and 6 in Figure 5 represented this process.

Assessment of the object separability and re classification

In order to assess the object separability among the training samples of the 2016 data, the object separation assessment was done by developing the application independently derived from the Jeffries Matusita (JM) distance formula (Gu et al., 2008; M. Dabboor et al., 2014). JM distance value ranges between 0 and 2.0. In general, the JM distance value separation criterion is categorized as good if > 1.9 and good enough if 1.7-1.9

(Gu et al, 2008; Dabboor et al, 2014; Sonobe et al, 2017).

The digital classification of time-series land cover were conducted using a spectral combination of correlation analysis, i.e., the four types of spectral band combinations consisted of the Bands 6-5-4-3-2, Bands 6-5-4, Bands 6-5-2, and Bands 6-5. From the digital classification of time-series land cover of all four spectral band groups, there were 20 annual mosaic image results analyzed using 24 classes of the land cover. The 20 images consist of 12 annual mosaic images classified by the same training samples, and eight annual mosaic images classified by independent training samples vary from year to year. The eight images were from four images in 2015 and four images in 2017. Each image was then re-classified into 16, 13, 9, 6, 4, and 2 classes so that it became 72 annual mosaic images. A total of 92 images was afterward analyzed to obtain the optimum accuracy results in the object separability using the confusion matrix. The results of re-classification using MLC of three-years data of 2015, 2016 and 2017 that processed by master training samples of 2016 were assessed with the confusion matrices and the JM distance analyses. The classification results were reclassified into 16, 13, 9, 6, 4, and 2 classes to improve the OA scores. The determination of the number and object classes to be re-classified referred to the results of the analysis of the JM distance matrix. Each the re-

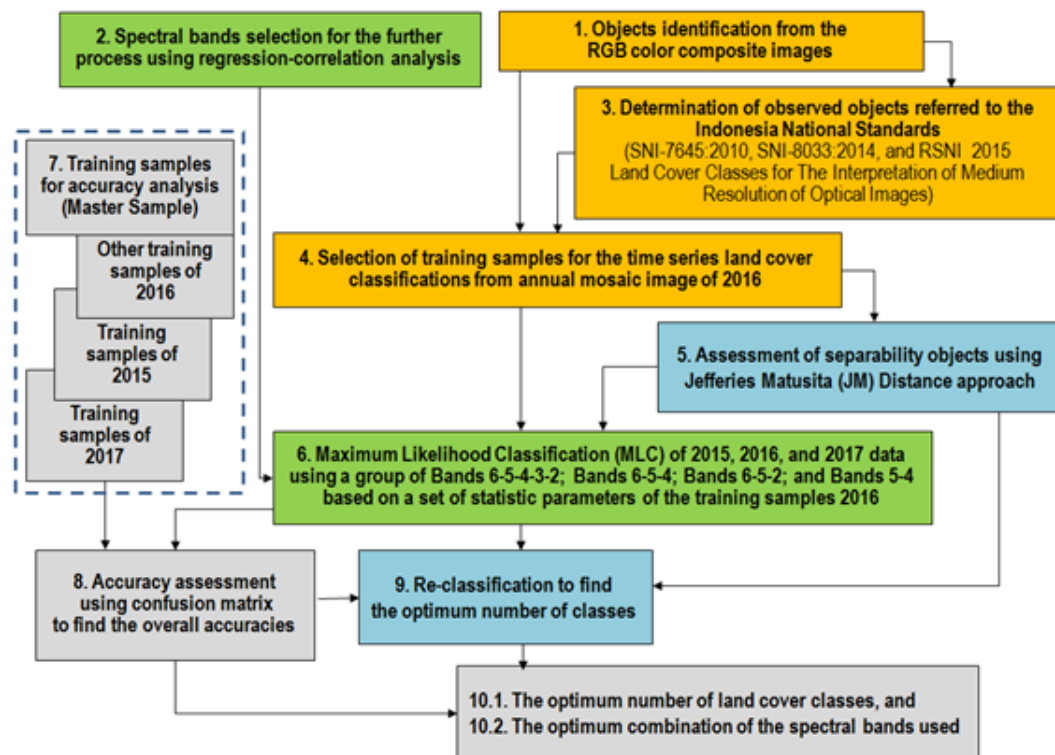


Figure 5. Procedure of the development steps of digital interpretability through digital time-series land cover classifications

classification step generated a confusion matrix. The steps of 5 and 9 in Figure 5 represented this process.

Accuracy assessment of the digital interpretability

In order to assess the OA, the independent training samples from three years data on the annual mosaic image of 2015, 2016 and 2017 were also generated. The training samples were captured at the different locations from the master training sample of the 2016 mosaic image. All three sets of training samples were used to perform the confusion matrix analysis, which were to conduct the assessment of accuracy using the OA (Peacock 2014; Sutanto 2013; Wulansari 2017). The OA assessments were made of a confusion matrix between digital analysis of time-series land cover based on sample 2016 with the training sample selected from the above three years data of 2015, 2016 and 2017. Finally, the analysis to determine the most optimal number of land cover classes and spectral band groups was proceeded with the criteria as below. The criteria of the number of land cover classes of each spectral band groups were determined based on the value of Average of Accuracy (AOA), namely (a) Good with value $>80\%$ or >0.80 , (b) Fair between $70.0\% - 79.9\%$ or $0.70 - 0.79$, and (c) Poor if $<70\%$ or <0.70 (Peacock 2014; Sutanto 2013). The number of land cover classes and the spectral band groups that meet the criteria of Good for all three years of data were recommended as the representation criteria for the digital analysis of time-series land cover using the annual mosaic image of Landsat-8 OLI data. The

steps of 7, 8, and 10 in Figure 5 represented this process.

However, for consideration of the efficiency and operationalization of the use of facilities and resources, such as storage space, processor, memory, speed and easiness of the process, the smallest number of land cover object classes and the smallest number of spectral bands used group that meet the criteria of Good for the three-years of data, were recommended for further digitally time-series land cover analysis using annual mosaic images. The optimal number of land cover classes and the optimal spectral band groups were recommended to be part of the regional and nationwide medium-scale remote sensing data standardization process.

3. Results and Discussions

Sample selection analysis

Based on the results of identification of land cover objects in an RGB image of 2016, with the support of Land Cover Map produced by MoEF of 2016 on the scale 1:250,000, and the field knowledge, the 24 land cover object classes were selected for the training samples for further classification processes. The determination of class types were also referred to the national standards of Land Cover Classes for the Interpretation of Medium Resolution of Optical Images 2010 and 2014 (BSN 2010, 2014, 2015). The training sample list of land cover objects and spectral signature values of each training sample are shown in Table 3 and Figure 6. From Table 3 and Figure 6, the objects of land covers by various vegetation had a similar spectral pattern at all spectral

bands. Therefore, the separation of the objects among vegetation cover types were not easy to complete. The training sample statistical parameters of the annual mosaic image of 2016 were calculated to analyze the object's separability and to classify the land cover from the annual mosaic image of 2015, 2016 and 2017. This was the beginning process of the digital interpretability, i.e. whether the training sample statistic parameters of the 2016 data could be used to classify time-series land cover of three-years data and resulting some adequate and acceptable AOA score of above > 0.80 .

Jeffries Matusita (JM) distance analysis was executed to compare the statistical separation among objects of the training samples (Dabboor et al, 2014; Sonobe et al, 2017). JM distance value ranges between 0 and 2.0. JM distance separation criterion is categorized as Very Good if > 1.9 and Good if 1.7-1.9 (Gu et al, 2008; Sonobe et al, 2017). In this study, the JM distance scores were multiplied by 1000 to make the difference between the JM distance scores looked more distinct. The results of the object separability assessment using JM distance, based on the statistical training samples of the annual mosaic image of 2016 for Bands 6-5-4-3-2 were shown in Table 4. In order to simplify the grouping of 24 classes of training sample objects observed, the author proposed five groupings of separability, i.e. very high, high, moderate, low, and very low, as shown in Table 5.

From the analyses of Tables 4 and 5, known that the objects belong to the very low separability or very difficult to distinguish from other objects were indicated by red shading, namely Dryland agriculture mixed with bush/shrub (TS-7), Swamp bush/shrub (TS-11), and Secondary inland forest (TS-15). The objects belong to the low separability or difficult to distinguish from other objects, were shown by pink shading, namely Estate forest (TS-1), Plantation (TS-3), Paddy field (TS-8), Grassland (TS-10), and Primary inland forest (TS-14).

The objects belong to the medium separability category ($<1600-1300$) or relatively easy to distinguish from other objects, were indicated by orange shading, namely Primary swamp forests (TS-4), Secondary swamp forests (TS-5), Bush/shrub (TS-6), Settlement-1 (TS-9), Primary mangrove forest (TS-19), Secondary mangrove forest (TS-20), and Other vegetated area or Tiling effect (TS-24). The objects that have high separability category or easily distinguishable from other objects were indicated by yellow shading, namely Airport area (TS-12) and Settlement-2 (TS-23). The dominant objects which had a very high separability category or very easily distinguished from other objects, indicated by green shading in succession of Open land-1 in the Estate forest or Plantation area (TS-2), Water body (TS-13), Cloud-1 or thick cloud (TS-16), Cloud-2 or thin cloud (TS-17), Cloud-3 or Cloud shadow (TS-18), Open land-1 in the mining area (TS-21), and Swamp (TS-22).

From the analysis results, it could be seen that

the separability of the land cover objects, which was analyzed using time-series data of 2015, 2016, and 2017 with group Bands 6-5-4-3-2, which categorized as very high or very easy to distinguish from other objects, namely Open land in Estate forest or Plantation area, Water bodies, Thick clouds, Thin clouds, Cloud shadow, Open land in the mining area, and Swamp. While the category of very low or the most difficult to distinguish from other objects, namely Dryland agriculture mixed with bush/shrub, Swamp bush/shrub, and Secondary inland forests.

Analysis of time-series land cover

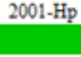
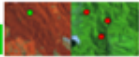

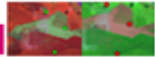
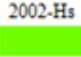

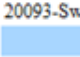
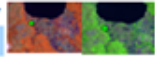
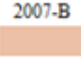
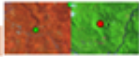


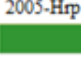

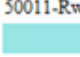
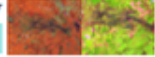
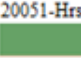

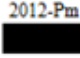
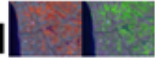
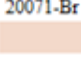

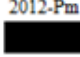

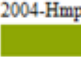
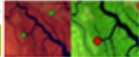
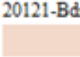
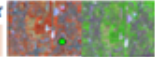
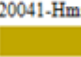
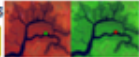
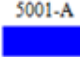

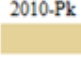
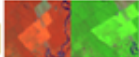
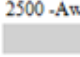

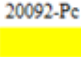
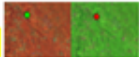
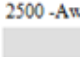
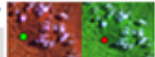
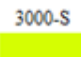

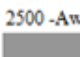

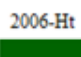

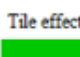

From the above analysis, it was found that the 24 classes indicates that not all of 24 land cover objects could easily be identified and differentiated each other, indicated by the average of the separation score of 4.3, requiring re-classification. The re-classification of the 24 land cover classes was carried out by analysis of the JM distance approach, and the re-classification staging scheme was shown in Figure 7. The 24 land cover classes were afterwards re-classified into 16, 13, 9, 6, 4, and 2 classes.

The rows of the confusion matrix show the results of the land cover classification based on the 2016 training sample, and the columns showing, training sample at different locations for the 2016, training sample of the annual mosaic image in 2015 and 2017. Two examples of the 92 confusion matrixes using the combination of the Bands 6-5-4-3-2 for 24 classes and six classes of land cover classification results based on the master training sample 2016 (rows) and training samples of 2016 at the different locations than those used in land cover classification (columns) are shown in Table 7. From Table 7 the OA of 24 land cover classes was 0.69 or 69%, and the OA of six land cover classes was 0.97 or 97%. The process of re-classifications of 24 classes into six classes were step-wisely executed through 16 classes, 13 classes, 9 classes, 6 classes, 4 classes, and 2 classes based on the results of the JM distance analysis in Figure 7. Each re-classification stage were calculated its OA by using the confusion matrix. As an example of 24 classes with the OA of 0.69 were re-classified into 16 classes, 13 classes, 9 classes, and 6 classes, and gradually increase the OA results of 0.79, 0.81, 0.92, and 0.97, respectively.

The six classes of land cover could also be identified from JM distance analysis, namely (1) Mixed dryland agriculture consisted of Dryland agriculture mixed with bush, Plantation, Bush/shrub, and Swamp bush/shrub; (2) Inland forest consisted of Secondary inland forest, Primary inland forest, and Estate forest; (3) Mangrove forest consisted of Primary mangrove forest, and Secondary mangrove forest; (4) Swamp forest consisted of Primary swamp forest and Secondary swamp forest; (5) Paddy field consisted of Paddy field and Grassland; and (6) Built-up area consisted of Airport areas, and Settlements.

While the use of the Bands 6-5-4, and Bands 6-5

Table 3. List of training sample (TS) of the observed land cover objects, extracted from the RGB 654 TBM image of 2016 scale 1:250.000*)

No	Class object	Training Sample Number (TS-X)	MoEF Map (Code and Symbol)	Feature in the RGB Image 564 654	No	Class object	Training Sample Number (TS-X)	MoEF Map (Code and Symbol)	Feature in the RGB Image 564 654
1	Primary inland forest	TS-14	2001-Hp 		13	Open land-1	TS-2	2014-T 	
2	Secondary inland forest	TS-15	2002-Hs 		14	Sawah (paddy field)	TS-8	20093-Sw 	
3	Bush/shrub	TS-6	2007-B 		15	Open land-2	TS-21	20141-Pb 	
4	Primary swamp forest	TS-4	2005-Hrp 		16	Swamp	TS-22	50011-Rw 	
5	Secondary swamp forest	TS-5	20051-Hrs 		17	Settlement-1	TS-9	2012-Pm 	
6	Swamp bush/shrub	TS-11	20071-Br 		18	Settlement-2	TS-23	2012-Pm 	
7	Primary mangrove forest	TS-19	2004-Hmp 		19	Airport areas	TS-12	20121-Bdr 	
8	Secondary mangrove forest	TS-20	20041-Hms 		20	Water body	TS-13	5001-A 	
9	Plantation	TS-3	2010-Pk 		21	Cloud-1 (thick)	TS-16	2500 -Aw 	
10	Dryland agriculture mixed with bush/shrub	TS-7	20092-Pc 		22	Cloud-2 (thin)	TS-17	2500 -Aw 	
11	Grassland	TS-10	3000-S 		23	Cloud-3 (shadow)	TS-18	2500 -Aw 	
12	Estate forest	TS-1	2006-Ht 		24	Other vegetated area (tile effect)	TS-24	Tile effect 	

Note:

- Open land-1: in the areas of Estate forest or Plantation
- Open land-2: in other areas, as well as mining area.

*) On the Display Monitor Screen

- Settlement-2: Similar to ordinary urban and built-up areas, but affected by cloud shadow;
- Brackish fishpond is categorized as Sawah (paddy field).

were accepted as well for the land cover classification with four classes resulted the AOA score of 0.86 or 86%. The four classes of land cover can be known from JM distance, namely (1) Vegetated land consisted of Primary swamp forest, Secondary swamp forest, Secondary inland forest, Primary inland forest, Dryland agriculture mixed with bush, Swamp bush/shrub, Plantation, Bush/shrub, Estate forest, Primary mangrove forest, Secondary mangrove forest, Paddy field, and Grassland; (2) Open land consisted of Open land either in the plantation or mining areas; (3) Water consisted of Water body, and Swampy

area; and (4) Built-up areas consisted of densely Settlement, Airport areas, and sparsely Settlement.

Based on the three-years' 2015, 2016, and 2017 time-series of land cover classification experiments, the achievements of OA and AOA of each class number resulted by land cover classifications using four types of the spectral band combinations were presented in the graphs of Figure 8. The annual mosaic image on tile 0.02 degrees indicated the consistency with Good accuracy (AOA of 86%) for the classifications up to six classes. Whereas the use of the Bands 6-5-4-3-2, Bands 6-5-4, and Bands 6-5 showed the consistent level of Good

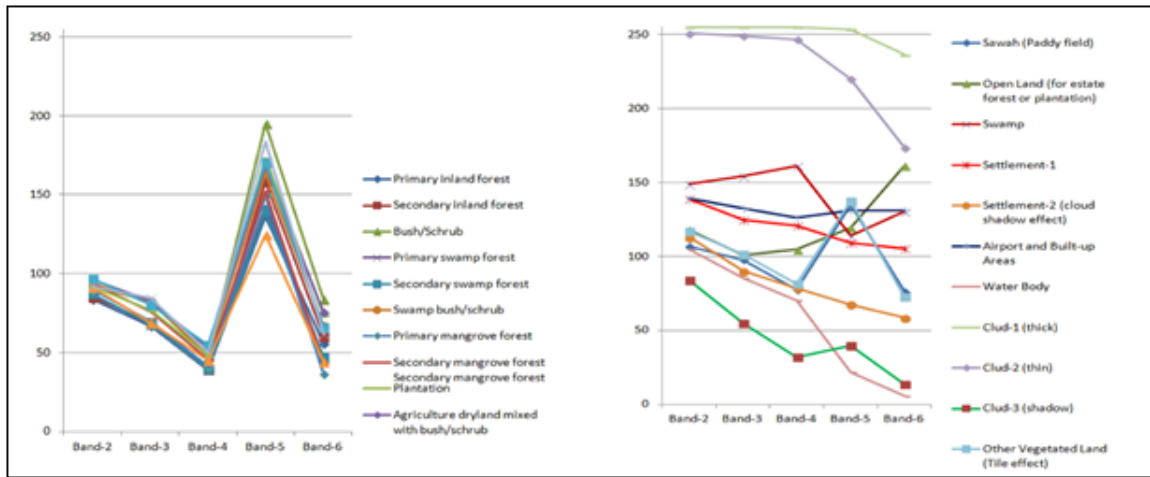


Figure 6. Spectral signature pattern of vegetation covered objects (left) and other objects (right) extracted from the training samples of 2016 mosaic data

Table 4. The JM of distance matrix the land cover training sample (TS) class objects

TS-	1	2	3	4	5	6	7	8	9	10	11	12	13	14	15	16	17	18	19	20	21	22	23	24	
1	0	1986	1556	1380	1319	1863	1426	1821	1908	1457	1423	1932	1999	1317	1165	2000	1999	1944	1103	1456	1997	1998	1911	1527	
2	1986	0	1990	1999	1999	1990	1943	1819	1740	1913	1944	1381	1999	1993	1997	1999	1999	1997	1997	1998	1969	1999	1959	1970	
3	1556	1990	0	1827	1791	859	604	1517	1930	1070	1154	1954	1999	1163	874	2000	1999	1999	1837	1868	1999	1957	1994	1693	
4	1380	1999	1827	0	233	1978	1771	1948	1994	1793	1720	1997	1999	1610	1197	2000	2000	1999	1612	1733	1999	1998	1999	1901	
5	1319	1999	1791	233	0	1951	1688	1912	1990	1770	1596	1996	1999	1465	1072	2000	2000	1997	1490	1645	1999	1976	1999	1865	
6	1863	1990	859	1978	1951	0	617	1501	1952	1499	812	1955	1999	1617	1356	2000	1999	1999	1938	1922	1999	1830	1996	1865	
7	1426	1943	604	1771	1688	617	0	1011	1798	1028	503	1827	1998	1298	1145	2000	1999	1977	1432	1412	1990	1690	1898	1429	
8	1821	1819	1517	1948	1912	1501	1011	0	1153	1567	1272	1398	1924	1635	1682	1999	1999	1956	1805	1845	1850	1834	1606	1042	
9	1908	1740	1930	1994	1990	1952	1798	1153	0	1889	1846	747	1994	1938	1969	1999	1999	1970	1976	1986	1690	1992	1169	1635	
10	1457	1913	1070	1793	1770	1499	1028	1567	1889	0	1403	1830	1999	1719	1559	2000	1999	1999	1253	1394	1997	1970	1984	1754	
11	1423	1944	1154	1720	1596	812	503	1272	1846	1403	0	1837	1985	1364	1318	2000	1999	1852	1418	1452	1987	1533	1852	1657	
12	1932	1381	1954	1997	1996	1955	1627	1398	747	1830	1837	0	1986	1966	1983	1999	1997	1965	1988	1995	1609	1998	1583	1827	
13	1999	1999	1999	1999	1999	1999	1998	1924	1994	1999	1985	1986	0	1999	1999	2000	1999	1898	1999	1999	1999	1999	1904	1988	
14	1317	1993	1163	1610	1465	1617	1298	1635	1938	1719	1364	1966	1999	0	590	2000	1999	1875	1785	1842	1999	1988	1962	1447	
15	1165	1997	874	1197	1072	1356	1145	1682	1969	1559	1318	1983	1999	590	0	2000	1999	1985	1465	1689	1999	1909	1996	1676	
16	2000	1999	2000	2000	2000	2000	2000	1999	1999	2000	2000	1999	2000	2000	2000	0	1695	2000	2000	2000	2000	2000	1999	1999	
17	1999	1999	1999	2000	2000	1999	1999	1999	1999	1999	1999	1999	1999	1999	1999	1695	0	1999	1999	1999	1999	2000	1999	1997	
18	1944	1997	1999	1999	1997	1999	1977	1956	1970	1999	1852	1965	1898	1875	1985	2000	1999	0	1937	1965	1999	1999	1776	1944	
19	1103	1997	1837	1612	1490	1938	1432	1805	1976	1253	1418	1988	1999	1785	1465	2000	1999	1937	0	830	1999	1853	1983	1877	
20	1456	1998	1868	1733	1645	1922	1412	1845	1986	1394	1452	1995	1999	1842	1689	2000	1999	1995	830	0	1999	1969	1997	1902	
21	1997	1969	1999	1999	1999	1999	1990	1850	1690	1997	1987	1609	1999	1999	1999	2000	1999	1999	1999	1999	1999	0	1999	1941	1988
22	1998	1999	1957	1998	1976	1830	1690	1834	1992	1970	1533	1998	1999	1988	1909	2000	2000	1999	1853	1969	1999	0	1999	1970	
23	1911	1959	1994	1999	1999	1996	1898	1606	1169	1984	1852	1583	1904	1962	1996	1999	1999	1776	1983	1997	1941	1999	0	1754	
24	1527	1970	1693	1901	1865	1865	1429	1042	1635	1754	1657	1827	1998	1447	1676	1999	1997	1944	1877	1902	1998	1970	1754	0	
Mean	1673	1938	1636	1769	1728	1717	1499	1656	1794	1689	1562	1815	1986	1677	1592	1986	1986	1959	1721	1779	1957	1933	1881	1771	
SD	310	418	551	532	539	542	563	451	488	457	498	473	406	491	530	410	410	404	480	465	412	411	430	430	
Rank	4	1	4	3	3	3	5	4	3	4	5	2	1	4	5	1	1	1	3	3	1	1	2	3	
TS-	1	2	3	4	5	6	7	8	9	10	11	12	13	14	15	16	17	18	19	20	21	22	23	24	

accuracy of up to four classes with the AOA of 89%, 82%, and 81%, respectively. Considering the of previous researches conducted by the consortium among LAPAN, MoEF, and Australia in the Indonesia Australia Forest Carbon Partnership (IAFCP), collaborative research between the University of Maryland and MoEF, and the research of MoEF itself, the results of this experiment provided more expectations. The digital classification approach for time-series land cover analysis of this

TBM image, for four objects classes, using three and two bands, resulted the AOA of 82% and 81%, respectively.

Since joint research of IAFCP that resulted Indonesia National Carbon Accounting System (INCAS), particularly for semi-automatic classification of the forests and non-forests changes for ten years (2000-2009), had the products with the lower accuracy of 78% (Wijaya et al, 2015). Although the collaboration research between the University of Maryland and MoEF, as well as the project of visual classification of land cover

by MoEF itself, produced the accuracies up to 90% and 98%, respectively. Those land cover classification researches were only up to two classes of forest and non-forest. For consideration of the operational efficiency of resource utilization, such as spacious storage, processor, memory, and the speed and easiness of process, the use of a combination of these three Bands 6-5-4 or two Bands 6-5 could be executed with a Good accuracy up to four classes of land cover analysis. Thus the TBM model is recommended to be part of the process of standardization of medium-scale remote sensing data.

Annual mosaic images

The results of the 2016 mosaic image for land cover classifications with MLC using the statistical parameters of the master training sample, for Bands 6-5-4-3-2 with 24, 16, 13, 9, 6, 4, and 2 classes were shown in Figure 9. While the example of the annual mosaic images of land cover with twenty four classes and re-classified into six classes of 2015, 2016, and 2017 were shown in Figure 10. From those figures, the objects separability of the four land cover classes was identified using JM distance, namely (1) Vegetated land, (2) Open land, (3) Water body, and (4) Built-up area were more easily distinguished among others in the annual mosaic image of 2015, 2016, and 2017. The above Vegetated land consisted of Primary swamp forest, Secondary swamp forest, Secondary inland forest, Primary inland forest, Dryland agriculture mixed with bush, Swamp bush/shrub, Plantation, Bush/shrub, Estate forest, Primary mangrove forest, Secondary mangrove forest, Paddy field, and Grassland. While the Open land consisted of Open land in the Estate forest or Plantation, and Open land in the mining and other areas. The Water Body consisted of Water Body and Swamp, and the Built-up area consisted of densely Settlement, Airport, and sparsely Settlement areas.

Based on the research findings, the annual mosaic images had Good digital interpretability. Therefore,

Rank (Class)	JM Distance Range	Σ	Score	Σ*Score
1	2000-1800	187	5	935
2	<1800-1600	30	4	120
3	<1600-1300	33	3	99
4	<1300-1000	16	2	32
5	<1000	10	1	10
	Σ	276		1196
Average = 1196/276 = 4.3				

Table 5. The categorization of the average of object separability based on JM distance

Table 6. The confusion matrix for measuring the overall accuracy (OA) of the 24 classes

Class	1	2	3	4	5	6	7	8	9	10	11	12	13	14	15	16	17	18	19	20	21	22	23	24	Σ	%		
1	5	17	7167	14758	855	0	130	17	0	12	144	0	5	5951	209	0	0	4	1636	500	0	0	18	4012	455166	92,17		
2	3206	127688	1217	1	0	4	129	292	259	94	221	118	0	0	0	0	0	0	0	0	0	0	4	0	139235	95,84		
3	22240	59	795126	4907	263	1804	7709	796	41	55	357	0	0	4930	1263	0	0	0	185	130	0	0	0	1138	841006	94,54		
4	5982	0	1195	160759	48051	0	47	1	0	0	152	0	0	14231	5823	0	0	0	270	62	0	0	0	11	1881420	96,08		
5	39869	0	1499	364630	34307	15	117	5	0	0	272	0	0	19816	544	0	0	0	1568	190	0	0	0	35	462892	7,41		
6	1136	4	144206	60	177	9556	8139	1323	16	37	3111	1	0	1207	1049	0	0	0	91	89	0	1	0	78	170287	5,61		
7	4417	827	69999	13519	648	508	10885	5476	222	186	448	15	14	1231	207	0	0	1	517	1072	0	0	41	1776	112016	9,72		
8	957	528	23535	192	60	331	15058	2291	75	45	24	1511	1439	259	0	0	12	377	48	6	0	126	6554	55387	27,19			
9	1114	1697	5849	1	2	0	57	1447	30276	6	3	180	31	22	0	0	1	0	0	2	0	2	791	502	41990	72,10		
10	3891	693	23921	738	641	115	1257	599	123	784	14	105	0	381	140	0	0	27	345	133	0	0	3	806	34726	2,26		
11	3341	186	15239	8171	2101	1648	7268	2651	24	43	3574	33	102	945	117	0	0	39	1414	474	0	10	29	566	47986	7,45		
12	2672	9919	7227	4	0	28	417	991	3308	92	145	599	440	55	6	12	8	12	0	2	13	0	99	99	26160	2,29		
13	0	1	127	0	0	1	0	59	0	0	0	0	307009	0	0	0	0	0	0	0	0	0	0	1	307211	99,93		
14	12034	3	33362	10407	439	45	596	254	5	11	61	0	0	257722	2914	0	0	25	353	105	0	0	6	4983	323339	79,71		
15	11142	4	430835	19847	1070	594	2949	135	0	20	254	0	2	109845	7974	0	0	0	1187	60	0	1	0	198	586132	1,36		
16	0	30	0	0	0	0	0	53	8	0	0	0	0	66	0	10493	593	0	0	0	0	0	0	0	11259	58,2		
17	0	6	19	16	0	0	0	192	66	0	0	5	56	323	0	357	1208	0	0	0	0	0	0	0	261	2526	47,82	
18	21	0	295	181	0	0	4	51	8	1	147	0	137	3816	0	0	0	5434	1	0	0	0	39	261	10464	52,41		
19	22086	0	637	19387	441	0	1372	95	0	2852	1195	0	9	400	13	0	0	36	54564	1705	0	1	4	36	105272	52,23		
20	4388	0	426	20899	2945	1	1113	146	0	895	535	0	0	248	2	0	0	0	25796	24994	0	0	6	8	82221	30,40		
21	0	56	219	0	0	0	0	115	291	0	0	8	5	1	0	0	0	0	0	0	0	0	401	0	4	1	1122	35,74
22	38	0	839	334	197	58	485	266	0	294	0	0	6	8	0	0	0	0	492	20	0	162	0	1	3222	5,03		
23	415	58	217	1	0	0	59	560	4929	0	3	45	2008	11	0	0	0	93	1	0	0	0	0	9181	289	17893	51,31	
24	5963	6	4705	2018	121	9	871	4763	656	0	31	0	16	6666	40	22	30	0	24	23	0	0	132	108414	134534	80,58		
Σ	564442	141782	1667861	2287662	90318	14717	45555	35345	42523	4963	11006	1133	311345	429312	20588	10384	1840	5733	89480	29607	422	175	10481	130030	5847466	47,60		
%	74,33	90,08	50,71	79,01	37,98	64,93	23,89	42,80	71,20	15,80	32,47	52,87	98,61	80,03	38,77	96,41	65,65	95,86	61,46	84,42	95,0292	3787,38	83,38	66,48	69,14			

Note:

The columns represented the training sample based on 2016 data; the rows represented the result of classification. The OA for 24 classes was 69%.

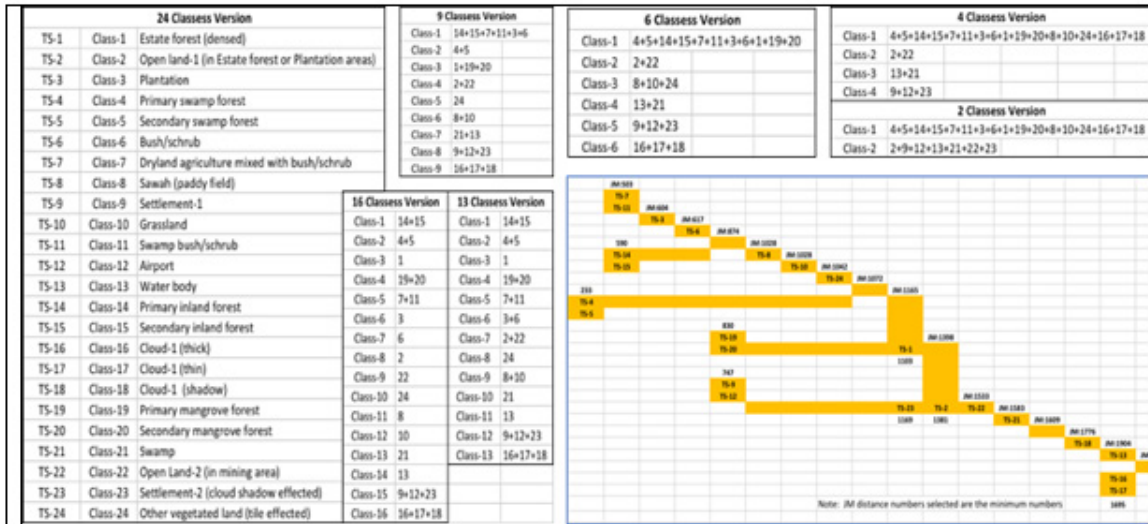


Figure 7. The scheme of the land cover re-classification analysis process

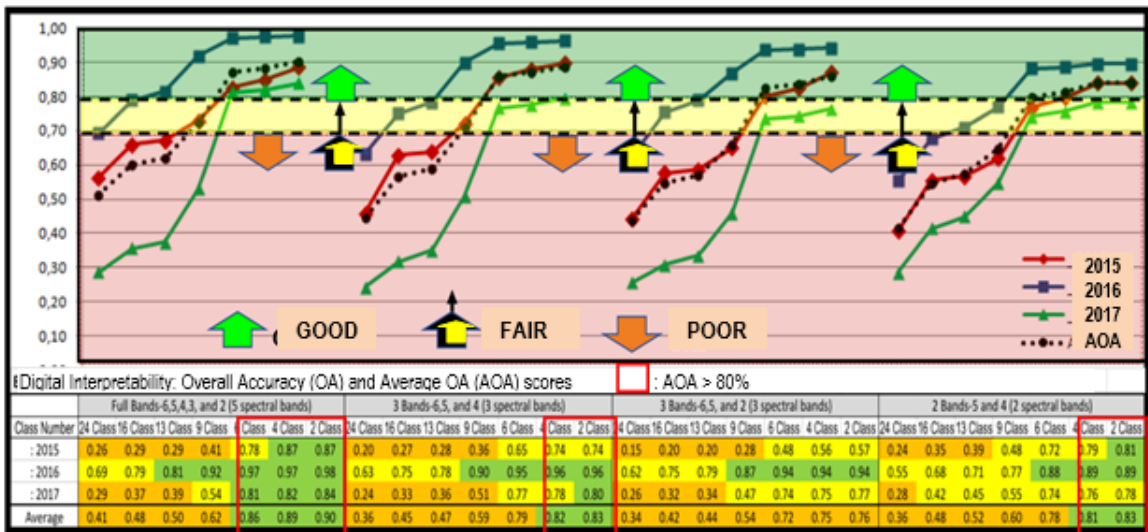


Figure 8. The achievements of OA and AOA of each class number resulted by land cover classifications using four types of the spectral band combinations

these data could be used for further digitally time series analysis, as well as visually interpretation (Dimiyati M. et al, 2018). It is expected that the TBM model would be effective in providing the needs of the remote sensing mosaic image of minimum cloud cover (Presiden of the Republic of Indonesia 2013, 2018) for medium scale analysis, such as national, provincial and regency levels, which is increasing in line with the increase of national development activities that implement One Map Policy (Presiden of the Republic of Indonesia 2011, 2013a, 2014a, 2018). Thus the need for annual mosaic images for areas often covered by clouds, such as Sumatra, Kalimantan, and Papua could be provided using the TBM images.

4. Conclusions

Deriving on the digital interpretability analysis of annual mosaic Landsat-8 OLI images for time-series

land cover of three-years data, with the case of the central part of Sumatra, it is concluded that the use of the Bands 6-5-4-3-2 performs the consistent accuracy level of the Good with the AOA score of 86% (> 80%) for six classes objects. Whereas the use of the Bands 6-5-4-3-2, Bands 6-5-4, and Bands 6-5 shows the consistent accuracy level of Good up to four class objects for the three-years' time-series land cover images of 2015, 2016, and 2017 with the AOA score of 89%, 82%, and 81%, respectively. It also means that the annual mosaic images have Good digital interpretability, providing an AOA score of 80% or above for six and four class objects. The TBM images are accepted for further digital land cover time series analysis.

Considering the operational efficiency of resource utilization, such as spacious storage, processor, memory, and the speed and easiness of the data

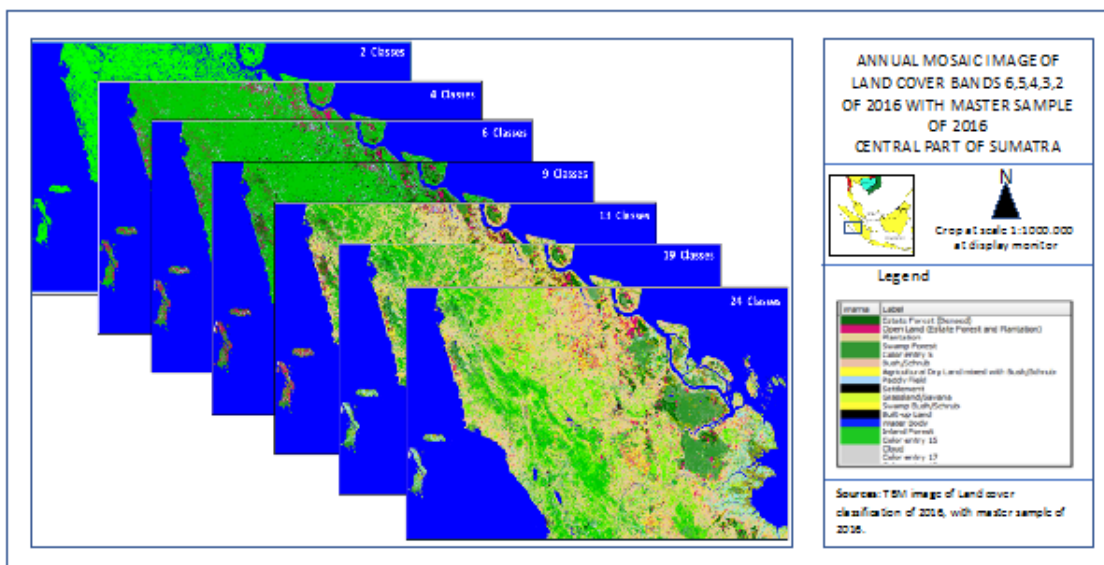
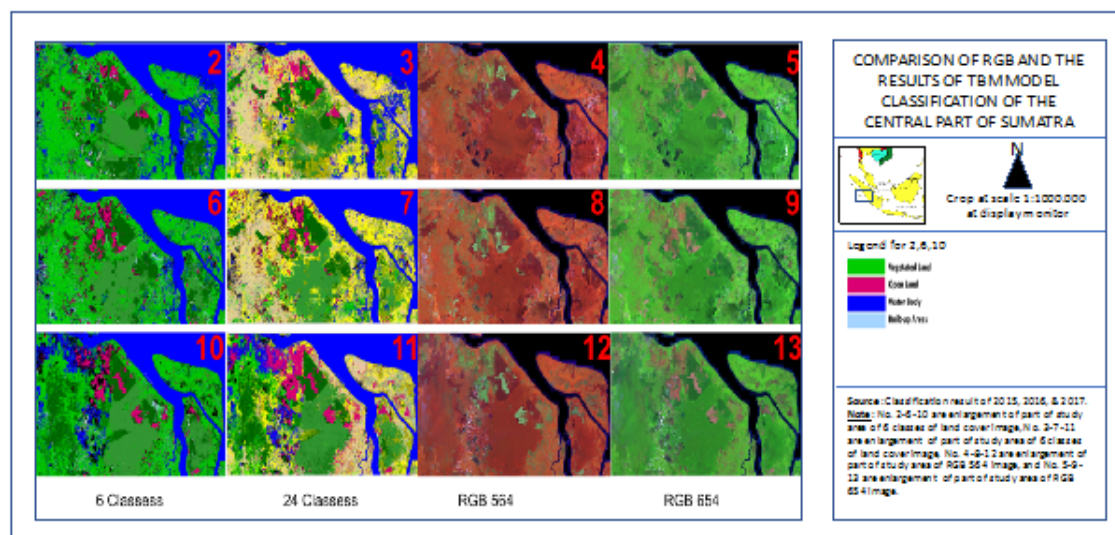


Figure 9. The land cover classification results with different class numbers using the group Bands 6-5-4-3-2 of the 2016 TBM images



Note:

The rows (up, down) representing the year of 2015, 2016, and 2017; the columns (right to left) representing RGB654, RGB 564, 24 and 6 classes.

Figure 10. The imageries of RGB and land cover classification results with 24 and 6 classes

processing, the most efficient for the time-series digital land cover analysis of an annual mosaic image is the use of a combination of the two Bands 6-5 for four classes. These four classes could be derived using JM distance analysis, namely Vegetated land, Open land, Water body, and Built-up areas.

Based on the above analysis, the annual mosaic image shows the consistent accuracy level for the classifications as well as the object separability of the land cover. Accordingly, the digital interpretability of annual mosaic images with tile size 0.02x0.02 degree is acceptable for further digital analysis of the object of time-series land cover. The development TBM data can be

recommended to be part of the standardization process of remote sensing data processing of medium scale analysis such as national, provincial and regency levels.

Acknowledgments

We are grateful to the all related institutions, especially Kemenristekdikti for the supports, Pustekdata LAPAN for providing data, image processing facilities, and coding or programming supports, and also to Faculty of Geography Gadjah Mada University team for scientific consultations, supports, and encouragements. We also thank colleagues from Pustekdata, LAPAN for working as a team, supporting

the data processing and parting the field observations, as well as all related support materials. Those are including Inggit Lolitasari, Kuncoro Adi Pradono, Syaiful Muflisin, and Randhy Prima Brahmantara.

References

- Andie Setiyoko, Riyan Mahendra Saputra, Abdul Asyiri, Gusti Dharma, & Yudha. (2016). Analisis Kesesuaian Pelayanan Data Penginderaan Jauh Terhadap Kebutuhan Pengguna (in Bahasa). In Seminar Nasional Penginderaan Jauh 2016 (pp. 424–527). Retrieved from www.lapan.go.id
- Badan Standardisasi Nasional (BSN). SNI 7645:2010: Klasifikasi penutupan lahan (in Bahasa), Pub. L. No. SNI 7645:2010, SNI 7645:228 (2010). Jakarta, Indonesia.
- Badan Standardisasi Nasional (BSN). SNI 8033:2014: Metode penghitungan perubahan tutupan hutan berdasarkan hasil penafsiran citra penginderaan jauh optik secara visual (in Bahasa), Pub. L. No. SNI 8033:2014, 9 (2014). Jakarta, Indonesia.
- Badan Standardisasi Nasional (BSN). RSNI-1 (2015): Kelas Penutupan Lahan dalam Penafsiran Citra Optis Resolusi Sedang (in Bahasa), Pub. L. No. RSNI-1 ICS, 17. Indonesia.
- Belinda Arunarwati Margono; Peter V. Potapov; Svetlana Turubanova; Fred Stolle; Matthew C. Hansen (2014). Primary forest cover loss in Indonesia over 2000–2012. *Nature Climate Change*, 4(August), 730–735. <https://doi.org/10.1038/NCLIMATE2277>
- Bodart, C., Eva, H., Beuchle, R., Raši, R., Simonetti, D., Stibig, H. J., Achard, F. (2011). Pre-processing of a sample of multi-scene and multi-date Landsat imagery used to monitor forest cover changes over the tropics. *ISPRS Journal of Photogrammetry and Remote Sensing*, 66(5), 555–563. <https://doi.org/10.1016/j.isprsjprs.2011.03.003>
- Broich, M., Hansen, M. C., Potapov, P., Adusei, B., Lindquist, E., & Stehman, S. V. (2011). Time-series analysis of multi-resolution optical imagery for quantifying forest cover loss in Sumatra and Kalimantan, Indonesia. *International Journal of Applied Earth Observation and Geoinformation*, 13 (2), 277–291. <https://doi.org/10.1016/j.jag.2010.11.004>
- Centre for Remote Imaging, Sensing and Processing (CRISP). (2001). Cloud-Free Mosaics. Retrieved March 9, 2017, from https://crisp.nus.edu.sg/~research/cloudfree_mosaic/cloudfree_mosaic.htm
- Costa, H., Foody, G. M., & Boyd, D. S. (2018). Supervised methods of image segmentation accuracy assessment in land cover mapping. *Remote Sensing of Environment*, 205 (December 2017), 338–351. <https://doi.org/10.1016/j.rse.2017.11.024>
- Costachioiu, T., Lazarescu, V., & Datcu, M. (2011). Classification of scene evolution patterns from satellite Image Time Series based on spectro-temporal signatures. ISSCS 2011 - International Symposium on Signals, Circuits and Systems, Proceedings, 305–308. <https://doi.org/10.1109/ISSCS.2011.5978721>
- Danoedoro, P. (2012). Pengantar Penginderaan Jauh Digital (in Bahasa) (First). Yogyakarta: Andi Offset.
- De Vries, C., Danaher, T., Denham, R., Scarth, P., & Phinn, S. (2007). An operational radiometric calibration procedure for the Landsat sensors based on pseudo-invariant target sites. *Remote Sensing of Environment*, 107(3), 414–429. <https://doi.org/10.1016/j.rse.2006.09.019>
- Dimiyati, R. D., Danoedoro, P., Hartono, Kustiyo (2018). A Minimum Cloud Cover Mosaic Image Model of the Operational Land Imager Landsat-8 Multitemporal Data using Tile based. *International Journal of Electrical and Computer Engineering*, 8 (1). <https://doi.org/10.11591/ijece.v8i1.pp360-371>
- Dimiyati M., Dimiyati RD, Kustiyo, Danoedoro P., Hartono. (2018). Interpretability Evaluation of Annual Multitemporal Tile Based Mosaic of Landsat-8 Operational Land Imager for Land Cover Changes Analysis in the Central Part of Sumatra. *Telkomnika*, Vol. 16/03 (June 2018), 1–14. <https://doi.org/http://dx.doi.org/10.12928/telkomnika.v16i3.9331>
- Furby, S. (2002). National carbon accounting system Land Cover Change Specification for Remote Sensing Analysis, Technical Report No. 9. Canberra.
- Furby, S. L., Caccetta, P. A., Wu, X., A., & Chia, J. (2006). Continental Scale Land Cover Change Monitoring in Australia using Landsat Imagery. CSIRO Mathematical and Information Sciences.
- Gastellu-Etchegorry, J. P. (1988). Monthly Probabilities For Acquiring Remote Sensed Data of Indonesia with Cloud Cover Less than 10, 20 and 30 Percent. *The Indonesian Journal of Geography*, 18 (55), 11–28.
- Ghosh, D., & Kaabouch, N. (2016). A survey on image mosaicing techniques. *Journal of Visual Communication and Image Representation*, 34, 1–11. <https://doi.org/10.1016/j.jvcir.2015.10.014>
- Gómez, C., White, J. C., & Wulder, M. A. (2016). Optical remotely sensed time series data for land cover classification: A review. *ISPRS Journal of Photogrammetry and Remote Sensing*, 116, 55–72. <https://doi.org/10.1016/j.isprsjprs.2016.03.008>
- Gu, J., Chen, J., Zhou, Q. M., Zhang, H. W., & Ma, L. (2008). Quantitative Textural Parameter Selection for Residential Extraction from High-Resolution Remotely Sensed Imagery. *The International Archives of the Photogrammetry, Remote Sensing and Spatial Information Sciences*. Vol. XXXVII. Part B4. Beijing 2008, Vol. XXXVI (2008), 1371–1376.
- Guo, Y., Li, F., Caccetta, P., And, D. D., & Berman, M. (2016). Cloud Filtering for Landsat TM Satellite Images Using Multiple Temporal Mosaicing. *IEEE IGARSS 2016*, 7240–7243.
- Hansen, M. C., & Loveland, T. R. (2012). A review of large area monitoring of land cover change using Landsat data. *Remote Sensing of Environment*, 122,

- 66–74. <https://doi.org/10.1016/j.rse.2011.08.024>
- Hansen, M. C., Roy, D. P., Lindquist, E., Adusei, B., Justice, C. O., & Altstatt, A. (2008). A method for integrating MODIS and Landsat data for systematic monitoring of forest cover and change in the Congo Basin. *Remote Sensing of Environment*, 112 (5), 2495–2513. <https://doi.org/10.1016/j.rse.2007.11.012>
- Islam, K., Jashimuddin, M., Nath, B., & Nath, T. K. (2016). Land use classification and change detection by using multi-temporal remotely sensed imagery: The case of Chunati wildlife sanctuary, Bangladesh. *Egyptian Journal of Remote Sensing and Space Science*, 21 (1), 37–47. <https://doi.org/10.1016/j.ejrs.2016.12.005>
- Kevin Butler. (2018). Band Combinations for Landsat 8. Retrieved from <https://blogs.esri.com/esri/arcgis/2013/07/24/band-combinations-for-landsat-8/>
- Kushardono, D., & Dewanti, R. (2016). Pemetaan Kebutuhan Sensor Optik Satelit Penginderaan Jauh di Indonesia (The Mapping of Remote Sensing Satellite Optical Sensor Needs in Indonesia) (in Bahasa). *Majalah Inderaja*, VII(9 Edisi November 2016), 20–27.
- Kustiyo. (2016). Development of Annual Landsat 8 Composite Over Central Kalimantan, Indonesia Using Automatic Algorithm to Minimize Cloud. *International Journal of Remote Sensing and Earth Sciences*, 13 (1), 51–58.
- Kustiyo, Dewanti, R., & Lolitasari, I. (2014). Pengembangan Metode Koreksi Radiometrik Citra SPOT 4 Multi-Spektral dan Multi-Temporal untuk Mosaik Citra. In *Seminar Nasional Penginderaan Jauh 2014* (pp. 79–87).
- Kustiyo, Roswintiarti, O., Tjahjaningsih, A., Dewanti, R., Furby, S., & Wallace, J. (2015). Annual forest monitoring as part of the Indonesia's National Carbon Accounting System. *International Archives of the Photogrammetry, Remote Sensing and Spatial Information Sciences - ISPRS Archives*, 40 (7W3), 441–448. <https://doi.org/10.5194/isprsarchives-XL-7-W3-441-2015>
- M. Dabboor; S. Howell; M. Shokr; J. Yackel. (2014). The Jeffries – Matusita distance for the case of complex Wishart distribution as a separability criterion for fully polarimetric SAR data. *International Journal of Remote Sensing*, 35(19), 6859–6873. <https://doi.org/10.1080/01431161.2014.960614>
- Ma, L., Li, M., Ma, X., Cheng, L., Du, P., & Liu, Y. (2017). A review of supervised object-based land-cover image classification. *ISPRS Journal of Photogrammetry and Remote Sensing*, 130, 277–293. <https://doi.org/10.1016/j.isprsjprs.2017.06.001>
- Margono, B. A., Usman, A. B., Budiharto, & Sugardiman, R. A. (2016). Indonesia's Forest Resource Monitoring. *Indonesian Journal of Geography*, 48(1), 7–20.
- Mausel, P. W., Kramber, W. J., & Lee, J. K. (1990). Optimum Band Selection for Supervised Classification of Multispectral Data, 56(1), 55–60.
- Mitchell, A. L., Milne, A., Tapley, I., Lowell, K., Caccetta, P., Lehmann, E., Held, A. (2011). Interoperability of radar and optical data for forest information assessment. *International Geoscience and Remote Sensing Symposium (IGARSS)*, 1397–1400. <https://doi.org/10.1109/IGARSS.2011.6049327>
- Mitchell A.L, Williams M, Tapley I, Milne A.K. (2012). Interoperability of Multi-Frequency SAR Data for Forest Information Extraction in Support of National MRV Systems. *IEEE IGARSS 2012*, 978-1-4673, 3166–3169.
- Mouginis-mark, P. J., Owensby, P., Chellis, C., & Lo, J. (2001). Cloud-Free Satellite Mosaics for Disaster Management, 00(C), 822–823.
- Roswintiarti Orbita, Ratih Dewanti, Furby Suzanne, Wallace Jeremy (2015). The Remote Sensing Monitoring Program of Indonesia's National Carbon Accounting System: Methodology and Products. Jakarta.
- Peacock, R. (2014). Land Cover Classification, Accuracy Assessment of Supervised and Unsupervised Classification Using Landsat Imagery of Little Rock, Arkansas. Northwest Missouri State University Master Thesis.
- Presiden Republik Indonesia. Undang-undang Republik Indonesia Nomor 4 Tahun 2011 tentang Informasi Geospasial (in Bahasa), No. NOMOR 4 TAHUN 2011 (2011).
- Presiden Republik Indonesia. Peraturan Pemerintah Republik Indonesia Nomor 8 Tahun 2013 tentang Ketelitian Peta Rencana Tata Ruang (in Bahasa), PP No 8 Tahun 2013 (2013).
- Presiden Republik Indonesia. Undang-undang Republik Indonesia Nomor 21 Tahun 2013 tentang Keantariksaan (in Bahasa), NOMOR 21 TAHUN 2013 (2013). Indonesia. Retrieved from www.lapan.go.id
- Presiden Republik Indonesia. Undang-undang Republik Indonesia Nomor 6 tahun 2014 tentang Desa (in Bahasa), Presiden Republik Indonesia (2014). <https://doi.org/10.1017/CBO9781107415324.004>
- Presiden Republik Indonesia. Undang Undang Republik Indonesia Nomor 20 Tahun 2015 tentang Standardisasi dan Penilaian Kesesuaian (in Bahasa) (2014). Indonesia.
- Presiden Republik Indonesia. Peraturan Presiden Republik Indonesia Nomor 9 Tahun 2016 tentang Percepatan Pelaksanaan Kebijakan Satu Peta pada Tingkat Ketelitian Peta Skala 1: 50.000 (in Bahasa), Pub. L. No. No 9 Year 2016 (2016).
- Presiden Republik Indonesia. Peraturan Pemerintah Nomor 11 Tahun 2018 tentang Tata Cara Penyelenggaraan Kegiatan Penginderaan Jauh, No. PP No 11 Tahun 2018, 45 (in Bahasa) (2018). Indonesia.
- Queensland Department of Science, Information Technology (2014). Land cover change in

- Queensland 2010–11: a Statewide Landcover and Trees Study (SLATS) report. Brisbane.
- Richards, J. A., & Jia, X. (2006). *Remote Sensing Digital Image Analysis, An Introduction 4th* (4th Editio). Canberra: Springer.
- Setiawan, Y., Lubis, M. I., Yusuf, S. M., & Prasetyo, L. B. (2015). Identifying Change Trajectory over the Sumatra's Forestlands Using Moderate Image Resolution Imagery. *Procedia Environmental Sciences*, 24, 189–198. <https://doi.org/10.1016/j.proenv.2015.03.025>
- Sonobe, R., Tani, H., & Wang, X. (2017). An experimental comparison between KELM and CART for crop classification using Landsat-8 OLI data. *Geocarto International*, 32 (2), 128–138. <https://doi.org/10.1080/10106049.2015.1130085>
- Sutanto (2013). *Metode Penelitian Penginderaan Jauh* (in Bahasa). Badan Penerbit Fakultas Geografi Universitas Gadjah Mada, Penerbit Ombak Yogyakarta.
- USGS. (2018). Landsat Missions How do Landsat 8 band combinations differ from Landsat 7 or Landsat 5 satellite data? USGS. Retrieved from <https://landsat.usgs.gov/how-do-landsat-8-band-combinations-differ-landsat-7-or-landsat-5-satellite-data>
- USGS. (2015). Landsat Mission, What are the best spectral bands to use for my study?
- Wijaya, A., Sugardiman, R. A., Budiharto, B., Tosiani, A., Murdiyarso, D., & Verchot, L. V. (2015). Assessment of large scale land cover change classifications and drivers of deforestation in Indonesia. *International Archives of the Photogrammetry, Remote Sensing and Spatial Information Sciences - ISPRS Archives*, 40 (7W3), 557–562. <https://doi.org/10.5194/isprsarchives-XL-7-W3-557-2015>
- Wulansari, H. (2017). Uji Akurasi Klasifikasi Penggunaan Lahan dengan Menggunakan Metode Defuzzifikasi Maximum Likelihood Berbasis Citra ALOS AVNIR-2 (in Bahasa). *Bhumi*, 3–No 1 (Mei), 98–110.
- Zhongyang, L., Zixuan, D., Huailiang, C., & Chunhui, Z. (2011). Study on the Land Use and Cover Classification of Zhengzhou Based on Decision Tree.